Ground state structure of $BaZrO_3$: A comparative first-principles study

Ante Bilić*
Materials Theory and Simulation Laboratory, Institute of High Performance Computing, 1 Fusionopolis Way, #16-16 Connexis 138632, Singapore

Julian D. Gale
Department of Applied Chemistry, Nanochemistry Research Institute, Curtin University of Technology, P.O. Box U1987, Perth 6845, Western Australia

(Received 10 February 2009; published 7 May 2009)

First-principles calculations, based on density-functional theory, are exploited to investigate the nature of the ground-state structure of barium zirconate. The experimentally observed simple-cubic structure is found to be dynamically unstable against an antiferrodistortive transformation. This instability manifests itself through imaginary frequency modes along the whole R-M edge of the Brillouin zone. The computations predict an orthorhombic crystal structure of the material, only slightly distorted from the cubic lattice, with an eight times larger unit cell and alternate ZrO_6 octahedra slightly rotated in opposite directions around the Cartesian axes. The apparent disagreement with some of the previous first-principles results regarding the nature of the ground-state structure is considered in detail. The neglect of the barium $5s^2$ and $5p^6$ electrons in the valence configuration of Ba is found to be responsible for the previously reported erroneous results.

DOI: 10.1103/PhysRevB.79.174107 PACS number(s): 77.84.Dy, 77.84.Bw, 71.15.Dx

I. INTRODUCTION

Ternary perovskite oxides comprise a large family of materials with the common ABO_3 general formula, though they exhibit a variety of structural phases, from cubic to rhombohedral, orthorhombic, tetragonal, and monoclinic.[1] Barium zirconate is a perovskite that is considered to have a perfect cubic structure[2] over a wide range of temperatures with a lattice constant of 4.19 Å.[3] Owing to the lack of observation of other structural phases with interesting properties, such as ferroelectricity,[4] $BaZrO_3$ has not received as much attention as other perovskites; most notably $BaTiO_3$.[5,6] However, in recent years new interest has arisen in barium zirconate spurred on by its desirable properties as a high-temperature proton conductor (HTPC),[7] a dielectric material for use in wireless communications applications,[8] and as a substrate for thin-film growth.[9] A recent study[10] combined first-principles computations and an effective Hamiltonian model with experimental efforts to investigate structural and dielectric properties of $BaZrO_3$. It concluded that, unlike most perovskites, $BaZrO_3$ does not undergo any structural phase transitions, remaining cubic and paraelectric down to 2 K. Interestingly, recent first-principles density-functional theory (DFT) calculations have consistently demonstrated a potential structural instability, clearly manifested through imaginary frequency optical modes at the R-point in the phonon spectrum.[10–12] As a consequence of the zone-boundary instability, at a sufficiently low temperature the crystal is expected to break symmetry and undergo the antiferrodistortive (AFD) transformation.[13] The distorted structure involves doubling of the primitive unit cell in each direction and three-dimensional tilting of the ZrO_6 octahedra, which then corresponds to an $a^-b^-c^-$ tilted perovskite in the notation of Glazer.[14]

The apparent disagreement between the experimental observations and theoretical predictions, as has been hypothesized, could be suppressed by the quantum zero-point vibrations[10,11,15] and/or the stabilization of the soft modes by anharmonic effects at finite temperature.[16] An additional problem was that earlier theoretical calculations predicted a substantially larger dielectric constant than has been measured[10] at low temperatures. Subsequently, another DFT study[12] demonstrated that this problem was related to the cubic structural model and that the discrepancy can be fully rectified if, instead of the cubic form, a distorted structure is adopted as the ground state of $BaZrO_3$ as obtained by removal of the imaginary modes. Hence, it was suggested[12] that the low-temperature x-ray diffraction and neutron-scattering experiments[10] could not detect the tilting of octahedra because the symmetry breaking was largely confined to oxygen, and the atomic form factor for O is rather low.

In recent years first-principles DFT calculations of the ion mobility in perovskite materials have gained momentum.[17,18] Gomez *et al.*[19] looked into the causes and effects of octahedral tilting on the energy landscape for proton mobility in barium zirconate and several other pseudocubic perovskite oxides. However, they found that $BaZrO_3$ remains cubic, unlike the other perovskites. In the work of Björketun *et al.*, similar DFT calculations have been used to model proton diffusion in a doped $BaZrO_3$,[20,21] to study the thermodynamics of doping and defect formation in $BaZrO_3$,[21,22] and also the vibrational properties of a doped $BaZrO_3$.[21,23] Here no distortions from the cubic structure were either reported or observed.[24] Around the same time Martinez *et al.*[26] calculated from first principles the enthalpies of formation for a range of ternary oxides, again reporting the cubic structure for $BaZrO_3$. At this point it is worth noting that Gomez *et al.*, Björketun *et al.*, and Martinez *et al.* all utilized the same implementation of density-functional theory; namely, the VASP package.[27,28] The cubic ground state for $BaZrO_3$ was also reported in another DFT study,[29] while the study that followed[15] reported a distorted structure, with a significant dependence of the tilt angle on the cell volume, thus adding

to the controversy. In some cases only the possibility of the cubic ground state was considered.[30–32]

The present paper reports a systematic investigation of structural and vibrational properties of barium zirconate using DFT as implemented in three different numerical implementations and, in particular, as a function of the quality of the pseudopotential approximation made. We find that the cubic form of $BaZrO_3$ is predicted to be dynamically unstable within density-functional theory, based on several widely used functionals, in agreement with previous studies.[10–12] Possible reasons for the erroneous observation of a stable cubic structure are discussed as well as the implications for the previously reported results. The ways to recover correct results from several previous studies that predicted the cubic structural model of $BaZrO_3$ and to avoid potential pitfalls in the future are suggested.

II. METHODS

Here we report a first-principles investigation of the $BaZrO_3$ crystal structure based on Kohn-Sham density-functional theory. The DFT computations were conducted using three widely used programs for materials modeling: PWSCF (Ref. 33) from the Quantum Espresso package,[34] VASP, and SIESTA.[35,36]

A. PWSCF

PWSCF employs a plane-wave basis set for the expansion of the Kohn-Sham orbitals. Ultrasoft pseudopotentials[37] for the description of the electron-ion interactions were used in the present work. Electron-electron exchange and correlation interactions were accounted for through the use of the functional of Perdew and Wang (PW91) (Ref. 38); a form of generalized gradient approximation (GGA). Consistent with the choice of the functional, the pseudopotentials for Ba, Zr, and O generated with the use of PW91 and provided at URL http://www.pswcf.org/pseudo.htm were utilized. To test the effects of the use of the local-density approximation (LDA) the parameterization of the exchange-correlation energy by Perdew and Zunger (PZ) (Ref. 39) has also been used. This, however, involved a slight inconsistency in the sense that the same pseudopotentials were used as in the case of GGA. An energy of 500 eV (36.8 Ry) was set as the cutoff for the plane-wave expansion, which is close to the upper bound of the range (20–40 Ry) suggested for the use with the O pseudopotential by its author (Axel Kohlmeyer). To verify that this value is sufficiently high a test of convergence of total-energy differences vs the energy cutoff has been carried out by evaluating the total energy of the cubic unit cell vs lattice constant. A subsequent fit to the Murnaghan equation of state produced lattice constants of 4.209, 4.205, 4.207, and 4.204 Å, with corresponding bulk moduli of 146, 150, 150, and 151 GPa, for cutoff energies of 300, 408, 500, and 545 eV, respectively. An equivalent plane-wave cutoff of 300 Ry was used to represent the charge density. Brillouin-zone integrations have been performed on a $6\times6\times6$ k-point Monkhorst-Pack mesh and with Gaussian smearing. To verify that this mesh is sufficiently dense a test of convergence of the total energy has been conducted. For the $2\times2\times2$, $4\times4\times4$, $6\times6\times6$, and $8\times8\times8$ grid the total energies of the cubic unit cell relative to that at the $10\times10\times10$ grid are 0.386, 0.008, 0.0005, 0.0003 eV, respectively. These tests confirm that an adequate convergence of both the energy differences and total energy is achieved with the energy cutoff of 500 eV and $6\times6\times6$ k-point grid. Response function calculations, based on density-functional perturbation theory (DFPT) (Ref. 40), were used to evaluate phonon spectra. Dynamical matrices were calculated on a $4\times4\times4$ mesh.

B. VASP

As for PWSCF, VASP also employs a plane-wave basis set to expand the Kohn-Sham eigenstates. The PW91 functional was again employed to describe electron-electron exchange and correlation interactions. Electron-ion interactions were accounted for through the use of both ultrasoft pseudo-(USP) potentials[41] and the projector augmented wave (PAW) method.[42,43] For oxygen two choices of USP potentials, the "soft" and "standard," and three choices of PAW potentials, the "soft," "standard," and "hard" are supplied with the distribution. The energy cutoff of the basis set is dictated by the O potential, which is harder than its Ba and Zr counterparts. In most computations we used the recommended upper bound from the O potential: 270, 400, 250, 400, and 700 eV, in the case of the soft-USP, standard-USP, soft-PAW, standard-PAW, and hard-PAW, respectively. However, for phonon calculations we found that these cutoffs may not be sufficient and can lead to unconverged results, especially when considering soft modes. More reliable results for these were obtained only when we requested "high-precision" computations, which required energy cutoffs 30% above the recommended upper limits: 338, 495, 313, 500, and 875 eV for the soft-USP, standard-USP, soft-PAW, standard-PAW, and hard-PAW O potentials, respectively. The effects of the use of the LDA have been inspected using the exchange-correlation energy as parameterized by Perdew and Zunger,[39] based on the correlation energies of Ceperley and Alder (CA),[44] in combination with the appropriate USP and PAW potentials, with cutoffs of 270 and 400 eV, respectively. In VASP the dynamical matrix is evaluated via central finite differences of the analytic first derivatives of the energy by displacing each atom along the three orthogonal Cartesian directions, followed by subsequent mass weighting. The eigenvectors and eigenvalues of this matrix define the vibrational normal modes and the associated frequencies. Unfortunately only the zone center (Γ-point) modes can currently be readily calculated from VASP. Hence, to address the issue of a potential dynamic instability at the R-point in the Brillouin zone of the unit cell, the relevant vibrational calculations had to be carried out for a $(2\times2\times2)$ supercell.

C. SIESTA

In the SIESTA methodology a linear combination of atomic orbitals (LCAO) is used to expand the Kohn-Sham wave functions. Nuclei and core electrons are replaced by norm-conserving pseudopotentials in fully separable form.[45] The scheme of Troullier and Martins[46] was exploited to generate the pseudopotentials, with scalar relativistic corrections in-

cluded for barium and zirconium. The reference atomic valence configurations for the construction of the pseudopotentials were the following: Ba $5s^2 5p^6 5d^0 4f^0$, Zr $4s^2 4p^6 4d^2$, (i.e., ionic configurations with a +2 charge), and O $2s^2 2p^4$. The inclusion of the semicore electrons, i.e., 5*s* and 5*p* of Ba and 4*s* and 4*p* of Zr is needed owing to the sizeable overlap of these shells with the conventional valence states. For electron-electron exchange and correlation interactions the PBE functional,[47] a form of GGA, was used for both pseudopotential generation and in the SIESTA calculations. For the purpose of direct comparison with the results from PWSCF and VASP, the PW91 functional was also examined. In addition, the GGA functional of Wu and Cohen (WC) (Ref. 48) was tested because it reproduces the experimental lattice parameters for ABO_3 more accurately than other available functionals.[49]

The one-electron Kohn-Sham eigenstates were expanded in a basis of strictly localized[50] numerical pseudoatomic orbitals.[51] Basis functions were obtained by finding the eigenfunctions of the isolated atoms enclosed within a soft confined spherical potential.[51] A split valence scheme was used to generate a single-ζ basis for the semicore states of Ba and Zr, and a double-ζ basis for the conventional valence states of all the atoms. For oxygen a polarization function was included, while for Zr and Ba the lowest lying unoccupied *p* state was added to the basis set. The previously optimized basis sets from the work of Junquera *et al.*[52] on $BaTiO_3$ were used for Ba and O. The Zr basis set was obtained for the cubic bulk ZrO_2 structure using a simplex search to minimize the total energy with respect to key basis set parameters.[25]

An auxiliary real space mesh was used to evaluate terms involving the charge density. An equivalent plane-wave cutoff of 450 Ry was used to represent the density. The integrals in reciprocal space were again found to be well converged using a $6\times6\times6$ Monkhorst-Pack grid for the unit cell. For the $(2\times2\times2)$ supercell of $BaZrO_3$ a $4\times4\times4$ *k*-point mesh was used.

Vibrational spectra were evaluated within the harmonic approximation. The force-constant matrix of the system was determined through central finite differences of the analytic first derivatives by displacing each atom by 0.04 a.u. along the three orthogonal Cartesian directions. A $(3\times3\times3)$ supercell geometry has been employed for these computations and a $2\times2\times2$ *k*-point grid. By applying phase factors to the force constants obtained within this larger cell it is possible to obtain the phonon dispersion.

III. RESULTS AND DISCUSSION

A. PWSCF

The optimum lattice constant computed from PWSCF using the PW91 functional is 4.207 Å, in very good agreement with the experimental value and a previous GGA calculation,[30] while exceeding LDA calculated values, which typically lie in the region of 4.157 Å.[4,12,15] The calculated contribution to the dielectric constant from electronic polarizability ε_∞ is 4.8, slightly below the values 4.93 and 4.94 recently reported,[10,12] and above 4.559 evaluated previously.[31] Calculated Born effective charges Z^* are 2.75, 6.05, −4.84, and −2.05 for Ba, Zr, O longitudinal, and O transversal displacements, respectively, in good agreement with those of Zhong *et al.*[53] The calculated phonon band structure is shown in Fig. 1. While the shape of the bands generally matches well those from the previous two studies,[10,12] there are some important differences to note. First, the R-point instability at an imaginary frequency of $118i$ cm^{-1} here appears much more prominent. This is the well-known R_{25} mode that corresponds to the rotation of ZrO_6 octahedra around all three Cartesian axes. Second, another dynamic instability manifests itself at the M-point through a normal mode with an imaginary frequency of $90i$ cm^{-1}. This particular instability has not been reported before for $BaZrO_3$, although the trend of softening of the optical mode at the M-point is evident in the study of Bennet *et al.*[12] when compared with the results of Akbarzadeh *et al.*[10] As a matter of fact, such an instability has been reported in the related system of $CaSiO_3$.[54] This mode, known as M_2, involves the rotation of oxygen octahedra around the [100] direction. For both $BaZrO_3$ and $CaSiO_3$ this instability extends along the whole R-M edge of the zone boundary.

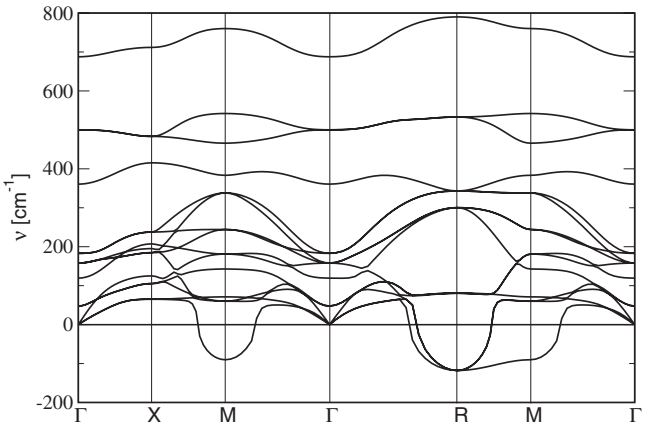

FIG. 1. Phonon dispersion curves for $BaZrO_3$ calculated by PWSCF using the PW91 functional.

B. VASP

The optimum lattice constants computed from VASP are 4.270, 4.288, 4.250, 4.250, and 4.252 Å based on the use of the soft-USP, standard-USP, soft-PAW, standard-PAW, and hard-PAW O potentials, respectively, in combination with the PW91 functional. It is interesting that these values slightly exceed the lattice constant obtained from most first-principles studies, with the exception of Björketun *et al.*[20] who reported the identical value (4.250 Å) using the same PAW potentials with VASP. Because only the Γ-point normal modes can be calculated from VASP, the phonon spectra were computed in the $2\times2\times2$ supercell using the calculated lattice constants. This geometry would allow the zone boundary (such as R-point and M-point) instability from the unit cell, if present, to manifest itself at the zone center of the supercell.

A total of three, forty five(sic), five, four, and three imaginary modes were found to exist using the soft-USP, standard-

USP, soft-PAW, standard-PAW, and hard-PAW O potentials, respectively, using the recommended energy cutoff for the plane-wave basis. The imaginary frequency ranges were 14–16, 44–327, 11–47, 6–44, and 17–18 cm^{-1}, respectively. We have investigated the nature of all of these modes by superimposing their eigenvectors onto the cubic structure. The distorted structures were then fully optimized. In the case of soft-USP and hard-PAW O potential, the structures with the three soft modes, while initially appearing ferroelectric (FE), all eventually resulted in the cubic geometry. Hence, they were merely the three acoustical modes contaminated by numerical noise that made them appear imaginary. In the case of the standard-USP O potential, after inducing the 45 soft modes in the cubic lattice, a variety of distortions could be observed, from FE to AFD and many others that could not be easily classified. However, subsequent optimization resulted in the perfect cubic geometry in all 45 cases. In the case of the soft-PAW potential, of the five soft modes, the three with frequencies $11i$ (doubly degenerate) and $15i$ cm^{-1} had a FE appearance but restored the structure to the cubic form after optimization. In contrast, when the two lowest lying modes, at $26i$ and $47i$ cm^{-1} and of the AFD nature, were optimized, their softness was confirmed by the optimized structures that clearly exhibit the AFD transformation. Finally, in the case of the standard-PAW potential, of the four "soft" modes, the two with frequencies $6i$ and $9i$ cm^{-1} had a FE appearance but reverted to the cubic form after optimization. Another lower lying mode, at $22i$ cm^{-1}, initially exhibited a clear AFD nature, but it produced the cubic form when optimized. Finally, the lowest lying mode, at $44i$ cm^{-1}, was optimized and it was confirmed to be imaginary resulting in a final structure that clearly exhibits an AFD transformation.

Given the large number of imaginary frequency modes predicted by VASP (for the standard-USP O potentials in particular), while only a single truly soft mode was eventually confirmed (with the soft-PAW and standard-PAW O potentials), all the calculations were repeated with a higher degree of accuracy. This was achieved using 30% higher energy cutoffs and denser Fourier meshes. A total of three only slightly imaginary frequency (ca. 10 cm^{-1}) modes were then found to be present with all the O pseudopotentials, except in the case of soft-PAW, where an additional imaginary mode with a frequency of 22 cm^{-1} was obtained. As in the calculations of lower accuracy, upon optimization of the structures distorted from the cubic by the induction of these eigenmodes, the high-symmetry cubic structure was eventually restored in each case, except for the mode at $22i$ cm^{-1} obtained with the PAW-soft O potential. Although its frequency has increased (in a positive sense) in high-accuracy calculations, its soft AFD nature was confirmed once again.

C. SIESTA

The lattice constant computed from SIESTA using the PBE functional is 4.242 Å, closer to the values obtained from VASP than the experimental value or that evaluated from PWSCF. A greater degree of overestimation of the lattice parameter for a localized orbital method is to be expected due to the incompleteness of the basis set relative to a converged plane-wave expansion. Calculated Born effective charges Z^* are 2.58, 6.44, −4.99, and −2.02 for Ba, Zr, O longitudinal, and O transversal displacements, respectively, in qualitative agreement with those from PWSCF. The calculated phonon band structure is shown in Fig. 2. Note that the computed dispersion curves in this figure do not include the nonanalytic correction that leads to the LO-TO splitting, since the high-frequency dielectric constant cannot currently be obtained from SIESTA. In contrast, the results of DFPT shown in Fig. 1 include this term. Apart from the pronounced softening of optical modes at the Γ-point, due to the aforementioned factor, the dispersion curves of Fig. 2 are in good agreement with those in Fig. 1. Most importantly, the R-point instability at an imaginary frequency of $99i$ cm^{-1} is almost as prominent here as in the PWSCF calculation. In addition, the dynamic instability at the M-point, first observed in the PWSCF calculated phonon spectrum, manifests itself here as well, at $103i$ cm^{-1}. Likewise, the same dynamical instability extends along the whole M-R edge of the zone boundary.

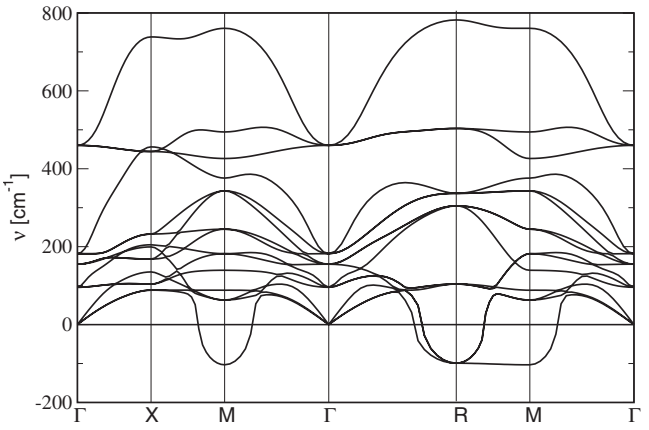

FIG. 2. Phonon dispersion curves for $BaZrO_3$ calculated by SIESTA using the PBE functional.

To evaluate the energy difference between the perfect cubic and distorted structure the calculated R_{25} soft mode was induced in the high-symmetry cubic structure and the $(2\times2\times2)$ supercell was then relaxed. The result was a low-symmetry orthorhombic structure with lattice constants $a=8.489$ Å, $b=8.477$ Å, and $c=8.468$ Å, i.e., the relaxed volume was 0.2% less than that of the high-symmetry structure. The octahedral tilt angle is 3.5°, in excellent agreement with previously reported values.[10,12] The R_{25} soft modes and optimized structure are illustrated in Fig. 3. The calculated difference in energy between the high- and low-symmetry structure was 4.4 meV per five atom stoichiometric unit, which is between the values of 1.5 and 8 meV reported previously.[10,12] However, as Kagimura *et al.* demonstrated,[15] the energy difference and ZrO_6 tilt angle are rather sensitive to the choice of lattice constant. It is worth noting that atom-centered basis sets, such as those used in the SIESTA methodology, are better suited for cell optimizations than plane-wave basis sets employed in a previous study[12] since there is no volume dependence of the basis set quality.

D. Analysis of the possible causes of discrepancies between previous studies

The present findings so far are completely consistent with those in the literature: VASP predicts a stable cubic structure

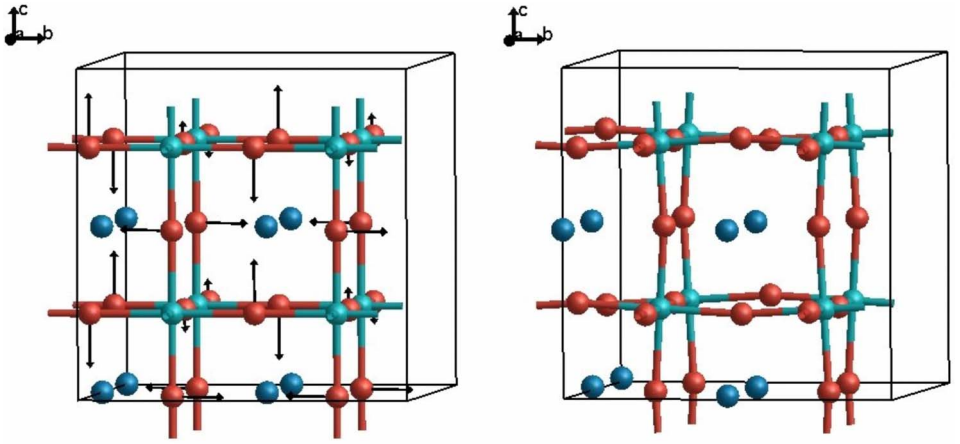

FIG. 3. (Color online) Left panel: the eigenvectors of the soft mode with the R_{25} symmetry. Note that the mode is triply-degenerate (along the three Cartesian directions). Right panel: the optimized structures of $BaZrO_3$ after the soft mode has been introduced in the cubic lattice.

for barium zirconate, while other apparently similar methods predict it to be dynamically unstable. One of the possible explanations for the apparent paradox is that different studies employed different exchange-correlation functionals, and no study so far has examined the influence of the choice of the functional. As a matter of fact, in all the previous studies that reported the dynamic instability in the cubic structure, only the LDA was employed, while in the VASP based studies only the GGA (PW91) was utilized.

To test the possible effects of the choice of exchange-correlation description on the structure of barium zirconate, a series of calculations were performed for the same numerical implementations with a number of different widely used functionals. The collated results are shown in Table I. The principal effect of the use of the LDA is, predictably, the reduction in the lattice constant and increase in the bulk modulus. It is interesting that the dynamic instabilities at the R and M points get more pronounced, as is evidenced by larger imaginary frequencies, in absolute magnitude, of the soft modes. However, with the present pseudopotentials and numerical conditions, VASP predicts no instabilities even with the use of the LDA. This suggests that the level of approximation in the electron exchange and correlation does not play a decisive role in the occurrence of the instability.

TABLE I. Collated results for the structure and properties of barium zirconate, as obtained from the programs PWSCF, VASP, and SIESTA. The VASP vibrational calculations were carried out in the $(2\times2\times2)$ supercell for the Γ point and with the high-precision settings (i.e., high energy cutoffs). In the vibrational frequency column, only imaginary modes are quoted.

Program	Exchange correlation functional	Pseudopotential	a [Å]	B_0 [GPa]	ν [i cm^{-1}]
PWSCF	PW91		4.207	150	118 (R), 90 (M)
PWSCF	PZ		4.138	172	152 (R), 122 (M)
PWSCF	PW91		4.1[a]		161 (R), 141 (M)
PWSCF	PW91		3.995[b]		199 (R), 180 (M), 40 (Γ)
PWSCF	PW91	Ba $5s^25p^6$ and Zr $4s^24p^6$ removed	4.398	166	
PWSCF	PW91	Ba $5s^25p^6$ removed	4.348	158	
PWSCF	PW91	Zr $4s^24p^6$ removed	4.287	157	154 (R), 139 (M)
VASP	PW91	O soft-USP	4.270	145	
VASP	PW91	O standard-USP	4.288	143	
VASP	PW91	O soft-PAW	4.250	148	22 (Γ)
VASP	PW91	O standard-PAW	4.250	147	
VASP	PW91	O hard-PAW	4.252	147	
VASP	CA	O soft-USP	4.190	172	
VASP	CA	O standard-PAW	4.176	181	
SIESTA	PBE		4.242	154	99 (R), 103 (M)
SIESTA	PW91		4.239	153	159 (R), 160 (M)
SIESTA	WC		4.201	168	81 (R), 80 (M)

[a]$BaZrO_3$ under a 12 GPa pressure.
[b]$BaZrO_3$ under a 31 GPa pressure.

Related to the effects of the use of the LDA, i.e., the reduced volume of the unit cell, at this point it is worth investigating the effect of the reduced volume under external hydrostatic pressure. This issue has already been considered in the context of ABO_3 perovskites by Magyari-Köpe *et al.*[55] Using a global parameterization method they concluded that a positive hydrostatic pressure stabilizes the less distorted structures (cubic in this case), whereas a negative pressure favors large octahedral rotations. In order to verify these findings in the case of $BaZrO_3$ we have evaluated phonon spectrum for the crystal at lattice parameters of 4.1 and 3.995 Å, as opposed to the equilibrium value of 4.207 Å, which correspond to applied pressures of 12 and 31 GPa, respectively. Contrary to previous findings, as Table I shows, this causes further softening of the unstable modes at the R and M points to $161i$ and $141i$ cm^{-1} at 12 GPa, and $199i$ and $180i$ cm^{-1} (in addition, an imaginary frequency mode arises at the Γ point, too) at 31 GPa. This result is also supported by very recent DFT calculations on $BaZrO_3$,[15] which clearly produce lower minimum energies and increasing octahedral rotation angles as the lattice parameter decreases.

A comparison of the results from three sets of SIESTA calculations with different GGA functionals in Table I is also interesting. It shows that PBE and PW91, expectedly, produce similar lattice parameter and bulk moduli. However, the use of the PBE functional actually results in a less unstable cubic structure. The significance of this finding is in the fact that the PAW potentials distributed with VASP, and therefore most widely used, correspond to three functionals; LDA (CA), PW91, and PBE. The latter have not been tested in this or in any previous studies. However, based on the SIESTA result, there would be little point in doing so, since PBE is expected to further stabilize the cubic structure, even more so than PW91. Consequently, there was no value in exploring the influence of the GGA functional within the VASP implementation since the cubic phase is already preferred. Finally, the use of the WC functional in SIESTA results in a very accurate lattice parameter, which is smaller than those that have been produced with all other GGA functionals. However, in contrast to the LDA calculations and the case of compressed crystal, here the imaginary frequencies have also decreased, though the qualitative behavior is as per the other GGA functionals.

Comparing the results from the VASP calculations in Table I it is clear that the accuracy and hardness of PAW and USP O potentials have little effect on the stability of the cubic structure. This leads to the hypothesis that the quality of the VASP Ba and Zr potentials, rather than that of O, is inadequate to reproduce the well established dynamic instability. The importance of quality of the transition-metal pseudopotentials in oxides has already been stressed, in particular for zirconates.[56] Unfortunately, the construction and refinement of pseudopotentials for use in VASP is not routinely performed by most users, leading to a reliance on the existing USP and PAW potentials provided. Therefore, in order to test whether the quality of the Ba and Zr potentials is the reason why the dynamically unstable $BaZrO_3$ cubic is not predicted by VASP, one actually has to use another program. For this purpose we have again used PWSCF and generated pseudopotentials for Ba and Zr in which their semicore electrons

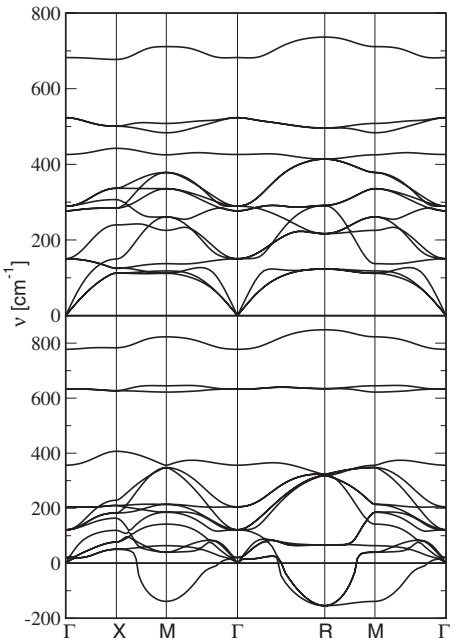

FIG. 4. Phonon dispersion curves for $BaZrO_3$ calculated by PWSCF using the PW91 functional. Upper panel: the semicore states of both Ba and Zr have been removed from the valence pseudopotential configurations. Lower panel: only the semicore states of Zr have been removed from the valence pseudopotential configurations.

$5s^25p^6$ and $4s^24p^6$, respectively, have been eliminated from the valence configuration and are accounted for only via a nonlinear partial core correction.[57] The cutoff radii for the partial core correction were set to 3.5 and 2.5 a.u. for Ba and Zr, respectively. Retaining the original O potentials and substituting these two potentials in PWSCF, PW91 calculations result in a significantly enlarged unit cell, with a constant of 4.398 Å and a reasonable compressibility, as shown in Table I. This lattice parameter indicates that the contribution to the bonding from the semicore electrons is substantial. However, the calculated phonon spectrum, shown in the upper panel of Fig. 4, exhibits no instabilities. This is a clear sign that the proper account of cation semicore states plays a vital role in the stability of the cubic structure.

To distinguish precisely which of the respective cation semicore states contributes to the instability, first the original Zr small-core pseudopotential was restored, while leaving the Ba and O potentials unchanged. This results in a slightly smaller lattice parameter of 4.348 Å, but still without a dynamical instability in the associated phonon spectrum (not shown). On the other hand, if the original Ba small-core pseudopotential is restored, while Zr potential is yet again replaced with the one that does not include the semicore states, the result is a substantially reduced lattice parameter of 4.287 Å, as shown in Table I. The associated phonon spectrum, illustrated in the lower panel of Fig. 4, clearly exhibits the R and M point instabilities. Hence, it is the proper account of barium valence electrons, rather than those of zirconium, that is critical for the occurrence of the instability. This finding is somewhat unexpected on the basis of previously discussed results for zirconates.[56] However, it is

plausible given that the 5*s* and 5*p* electrons have less core character than their counterparts in the fourth shell. Interestingly, Magyari-Köpe *et al.*[55] have previously found that the balance between the interaction of semicore states of the A and B cations with O ions effectively determines the adopted structure of the ABO_3 perovskites. The present findings suggest that, in the case of $BaZrO_3$, the semicore electrons of Zr seem to be less important than those of Ba, presumably owing to the more covalent (i.e., less ionic) character of the Zr–O bonds, arising from the presence of 4*d* electrons.

The VASP USP potential for Ba has an unusually large outermost core radius of 3.74 a.u., in contrast to 2.6 a.u. of its PWSCF counterpart and 2.5 a.u. of the norm-conserving SIESTA pseudopotential. Indeed, the $5s^2$ electrons are not even formally the part of the active valence configuration in the VASP Ba USP potential. The six 5*p* electrons are formally included in the valence configuration, but, given the large core radius, they may not be well described. These inadequacies in the treatment of the semicore electrons in the Ba USP potential explain why the results for $BaZrO_3$ are at odds with all other reported findings. On the other hand, the Ba PAW potential has an outermost core radius of 2.8 a.u. and includes both the 5*s* and 5*p* electrons in the valence configuration. Consequently, a much higher energy cutoff is recommended for the PAW than for the USP potential (187 vs 99 eV). Given the fact that PAW potentials are typically more accurate than the USP counterparts, it remains unclear why even the PAW account in VASP fails to predict the unstable cubic lattice for $BaZrO_3$.

E. Discussion

The results of the present work shed light on the controversy regarding the stability of the cubic $BaZrO_3$ lattice apparent in the published literature on this material. While the experimental structural investigations unanimously agree that the perfect cubic structure persists even down to cryogenic temperatures, the situation on the theoretical front has been far less clear. The majority of computational studies have reported a weak dynamical instability at the R-point. The result does not appear to be sensitive to the choice of the functional, basis set, or level of approximation in the treatment of the core electrons (i.e., whether a full potential or pseudopotential method is used). However, several computational investigations found no instability,[20–23,26] although in some cases they were concerned with its possible effects.[19]

The present results demonstrate that, in at least two cases[19,26] the reasons for this discrepancy lies with the quality of the USP potentials provided with the VASP code, which are optimized for efficiency, rather than accuracy and transferability. Of course we note that the ultimate responsibility always lies with the user to validate any approximations for their particular system of interest. Since the balance of the interactions of semicore states of the cations and oxygen ions is crucial for the proper account of bonding in perovskites,[55] the omission of the semicore states from the valence electron configuration in the VASP USP Ba potential explains the lack of observation of ZrO_6 tilting in those cases.

In other studies of $BaZrO_3$ that employed VASP (Refs. 20–23) the PAW potentials were employed which, according to our findings, can predict an elusive imaginary normal mode in the supercell geometry that corresponds to a zone-edge dynamic instability of the unit cell. However, this single mode appears to be much less soft than the modes predicted using other implementations and pseudopotentials. In addition, its softness is also dependent on the size of the basis set and can be completely lifted if a sufficiently high energy cutoff is used. Hence, it is likely that the instability was simply too weak to be observed, even though the lattice dynamics was investigated in the favorable geometry and with defects,[21,23] which should contribute to the symmetry lowering effects. Thus, the appropriateness of the present VASP PAW potentials for the structural and dynamical investigations of perovskites is, at best, dubious and users should be encouraged to generate more transferable pseudopotentials.

The present work predicts a dynamical instability in the $BaZrO_3$ lattice that is more profound than reported previously and that extends over a significant portion of the Brillouin zone. It is not clear what might be the reason for disagreement with previous investigations, which reported the instability confined to the R-point. However, the good agreement between the results in the present work obtained using two very different methods, PWSCF with plane-waves and DFPT vs SIESTA with LCAO and finite differences, provides additional confidence that our findings are correct. Indeed, analogous results were obtained for $CaSiO_3$.[54] The similarities in the calculated phonon spectra of $BaZrO_3$ and $CaSiO_3$ and in terms of geometrical considerations,[55] provide additional support for the current findings.

Finally, on the basis of the previous and current results it cannot be determined whether the ground-state structure of $BaZrO_3$ is cubic or pseudocubic. The only valid conclusion is that the cubic lattice is dynamically unstable, although potentially thermodynamically stable owing to quantum zero-point vibrations and the stabilization of the soft modes by anharmonic effects at finite temperatures. Considering that the amount of predicted octahedral tilting in $BaZrO_3$ is very small and limited to oxygen it would be very difficult to observe the distortion in experiment even at very low temperatures. At room temperature, where the cubic lattice is expected to be thermodynamically stable, inelastic neutron scattering would be the proper way of investigating the dynamic instability.[58]

IV. CONCLUSIONS

In the present work we have investigated the structure and phonon stability of cubic barium zirconate based on three popular numerical implementations of Kohn-Sham density-functional theory with a view to resolving current inconsistencies in the published literature. The vibrational spectra evaluated from PWSCF and SIESTA exhibit a dynamical instability at the R-point, in line with most previous studies. The system is predicted to favor ZrO_6 octahedral tilting, thereby lowering the symmetry. In addition, the instability manifests throughout the R-M edge of the zone boundary, which has not been previously reported. In contrast, the spectra evaluated with ultrasoft pseudopotentials provided with the widely

used VASP program do not exhibit any instability. This is a result of shortcomings of the Ba ultrasoft pseudopotential in particular, which excludes the $5s^2$ electrons from the semicore states and possesses a very large core radius, resulting in an inadequate account of the $5p^6$ electrons for this material. If, instead, the PAW potentials are employed in VASP, a weak instability can be reproduced, but even then the results are only marginally improved and remain at odds with those from small core norm-conversing pseudopotentials, as well as ultrasoft pseudopotentials within other implementations of DFT.

In conclusion, the study of barium zirconate serves as a cautionary tale for those using density-functional theory to study perovskite, as well as other oxide, materials. The examination of phonon instabilities and their consequences for structure symmetry is especially demanding of the quality of the pseudopotential being used and therefore validation against either small-core pseudopotentials, constructed to be transferable, rather than inexpensive, or full potential/all electron calculations should always be undertaken.

ACKNOWLEDGMENTS

We would like to thank the Australian Research Council for financial support through Discovery grants. The use of supercomputer facilities through the National Computational Infrastructure (NCI/APAC) service and iVEC is gratefully acknowledged. We thank M. E. Björketun and G. Wahnström for valuable discussions regarding their previous work.

*bilica@ihpc.a-star.edu.sg

[1] R. W. G. Wyckoff, *Inorganic Compounds* (Wiley, New York, 1964).
[2] H. D. Megaw, Proc. Phys. Soc. London **58**, 133 (1946).
[3] W. Pies and A. Weiss, in *Landolt-Börnstein: Numerical Data and Functional Relationships in Science and Technology*, edited by K.-H. Hellwege and A. M. Hellwege (Springer, Berlin, 1975), Vols. 7b1 and 7e.
[4] R. D. King-Smith and D. Vanderbilt, Phys. Rev. B **49**, 5828 (1994).
[5] R. E. Cohen and H. Krakauer, Phys. Rev. B **42**, 6416 (1990).
[6] W. Zhong, D. Vanderbilt, and K. M. Rabe, Phys. Rev. B **52**, 6301 (1995).
[7] K. D. Kreuer, Annu. Rev. Mater. Res. **33**, 333 (2003).
[8] M. T. Sebastian, *Dielectric Materials for Wireless Communication* (Elsevier, Amsterdam, 2008).
[9] P. S. Dobal, A. Dixit, R. S. Katiyar, Z. Yu, R. Guo, and A. S. Bhalla, J. Appl. Phys. **89**, 8085 (2001).
[10] A. R. Akbarzadeh, I. Kornev, C. Malibert, L. Bellaiche, and J. M. Kiat, Phys. Rev. B **72**, 205104 (2005).
[11] W. Zhong and D. Vanderbilt, Phys. Rev. Lett. **74**, 2587 (1995).
[12] J. W. Bennett, I. Grinberg, and A. M. Rappe, Phys. Rev. B **73**, 180102(R) (2006).
[13] G. A. Samara, T. Sakudo, and K. Yoshimitsu, Phys. Rev. Lett. **35**, 1767 (1975).
[14] A. M. Glazer, Acta Crystallogr. **28**, 3384 (1972).
[15] R. Kagimura, M. Suewattana, and D. J. Singh, Phys. Rev. B **78**, 012103 (2008).
[16] B. Magyari-Kope, L. Vitos, G. Grimvall, B. Johansson, and J. Kollar, Phys. Rev. B **65**, 193107 (2002).
[17] A. Bilić and J. D. Gale, Chem. Mater. **19**, 2842 (2007).
[18] A. Bilić and J. D. Gale, Solid State Ionics **179**, 871 (2008).
[19] M. A. Gomez, M. A. Griffin, S. Jindal, K. D. Rule, and V. R. Cooper, J. Chem. Phys. **123**, 094703 (2005).
[20] M. E. Björketun, P. G. Sundell, G. Wahnström, and D. Engberg, Solid State Ionics **176**, 3035 (2005).
[21] M. E. Björketun, P. G. Sundell, and G. Wahnström, Faraday Discuss. **134**, 247 (2007).
[22] P. G. Sundell, M. E. Björketun, and G. Wahnström, Phys. Rev. B **73**, 104112 (2006).
[23] M. Karlsson, M. E. Bjorketun, P. G. Sundell, A. Matic, G. Wahnstrom, D. Engberg, L. Borjesson, I. Ahmed, S. Eriksson, and P. Berastegui, Phys. Rev. B **72**, 094303 (2005).
[24] M. E. Björketun, private communication to A. Bilić.
[25] The pseudopotential for Zr and associated basis set can be downloaded from URL http://www.eminerals.org/siesta.
[26] J.-R. Martinez, C. E. Mohn, S. Stølen, and R. Søndenå, Phys. Chem. Chem. Phys. **8**, 2036 (2006).
[27] G. Kresse and J. Hafner, Phys. Rev. B **47**, 558 (1993).
[28] G. Kresse and J. Furthmüller, Comput. Mater. Sci. **6**, 15 (1996).
[29] M. Ghita, M. Fornari, D. J. Singh, and S. V. Halilov, Phys. Rev. B **72**, 054114 (2005).
[30] R. Terki, H. Feraoun, G. Bertrand, and H. Aourag, Phys. Status Solidi B **242**, 1054 (2005).
[31] R. Khenata, M. Sahnoun, H. Baltache, M. Rérat, A. H. Rashek, N. Illesa, and B. Bouhafs, Solid State Commun. **136**, 1054 (2005).
[32] N. Iles, A. Kellou, K. D. Khodja, B. Amrani, F. Lemoigno, D. Bourbie, and H. Aourag, Comput. Mater. Sci. **39**, 896 (2007).
[33] S. Baroni *et al.*, URL http://www.pwscf.org.
[34] http://www.quantum-espresso.org
[35] D. Sánchez-Portal, P. Ordejón, E. Artacho, and J. M. Soler, Int. J. Quantum Chem. **65**, 453 (1997).
[36] J. M. Soler, E. Artacho, J. D. Gale, A. García, J. Junquera, P. Ordejón, and D. Sánchez-Portal, J. Phys.: Condens. Matter **14**, 2745 (2002).
[37] D. Vanderbilt, Phys. Rev. B **41**, 7892 (1990).
[38] J. P. Perdew and Y. Wang, Phys. Rev. B **45**, 13244 (1992).
[39] J. P. Perdew and A. Zunger, Phys. Rev. B **23**, 5048 (1981).
[40] S. Baroni, S. de Gironcoli, A. Dal Corso, and P. Giannozzi, Rev. Mod. Phys. **73**, 515 (2001).
[41] G. Kresse and J. Hafner, J. Phys.: Condens. Matter **6**, 8245 (1994).
[42] P. E. Blochl, Phys. Rev. B **50**, 17953 (1994).
[43] G. Kresse and D. Joubert, Phys. Rev. B **59**, 1758 (1999).
[44] D. M. Ceperley and B. J. Alder, Phys. Rev. Lett. **45**, 566 (1980).
[45] L. Kleinman and D. M. Bylander, Phys. Rev. Lett. **48**, 1425 (1982).
[46] N. Troullier and J. L. Martins, Phys. Rev. B **43**, 1993 (1991).
[47] J. P. Perdew, K. Burke, and M. Ernzerhof, Phys. Rev. Lett. **77**,

3865 (1996).
[48] Z. Wu and R. E. Cohen, Phys. Rev. B **73**, 235116 (2006).
[49] S. R. Phillpot, S. B. Sinnott, and A. Asthagiri, Annu. Rev. Mater. Res. **37**, 239 (2007).
[50] O. F. Sankey and D. J. Niklewski, Phys. Rev. B **40**, 3979 (1989).
[51] J. Junquera, O. Paz, D. Sanchez-Portal, and E. Artacho, Phys. Rev. B **64**, 235111 (2001).
[52] J. Junquera, M. Zimmer, P. Ordejón, and P. Ghosez, Phys. Rev. B **67**, 155327 (2003).
[53] W. Zhong, R. D. King-Smith, and D. Vanderbilt, Phys. Rev. Lett. **72**, 3618 (1994).
[54] L. Stixrude, R. E. Cohen, R. Yu, and H. Krakauer, Am. Mineral. **81**, 1293 (1996).
[55] B. Magyari-Kope, L. Vitos, B. Johansson, and J. Kollar, Phys. Rev. B **66**, 092103 (2002).
[56] I. Grinberg, N. J. Ramer, and A. M. Rappe, in *Fundamental Physics of Ferroelectrics*, edited by H. Krakauer (American Institue of Physics, New York, 2001), p. 211.
[57] S. G. Louie, S. Froyen, and M. L. Cohen, Phys. Rev. B **26**, 1738 (1982).
[58] Y. Kuroiwa, A. Konishi, T. Shobu, Y. Noda, K. Fuchizaki, Y. M. Y. Y. Yamada, H. R. Child, H. Chou, and S. C. Moss, J. Phys. Soc. Jpn. **66**, 1033 (1997).